

Electronic Correlations Decimate the Ferroelectric Polarization of Multiferroic HoMn_2O_5

Gianluca Giovannetti^{1,2} and Jeroen van den Brink^{1,3}

¹*Institute Lorentz for Theoretical Physics, Leiden University, P.O. Box 9506, 2300 RA Leiden, The Netherlands*

²*Faculty of Science and Technology and MESA+ Research Institute, University of Twente, P.O. Box 217, 7500 AE Enschede, The Netherlands*

³*Institute for Molecules and Materials, Radboud Universiteit Nijmegen, P.O. Box 9010, 6500 GL Nijmegen, The Netherlands*

(Received 5 February 2008; published 5 June 2008)

We show that electronic correlations decimate the intrinsic ferroelectric polarization of multiferroic manganites RMn_2O_5 , where R is a rare earth element. Such is manifest from *ab initio* band structure computations that account for the Coulomb interactions between the manganese $3d$ electrons—the root of magnetism in RMn_2O_5 . Including these leads to an amplitude and direction of polarization of HoMn_2O_5 that agree with experiment. The decimation is caused by a near cancellation of the ionic polarization induced by the lattice and the electronic one due to valence charge redistributions.

DOI: 10.1103/PhysRevLett.100.227603

PACS numbers: 77.80.-e, 71.10.-w, 71.27.+a, 71.45.Gm

Introduction.—Multiferroics, single phase compounds in which magnetism and ferroelectricity coexist, are rare [1–3]. These materials, such as for instance the manganites RMn_2O_5 ($R = \text{Ho}, \text{Tb}, \text{Y}, \text{Eu}, \text{etc.}$) [4–10], are currently of great interest because of the possibility to control *magnetic* properties by *electric* fields and vice versa. It was recently discovered that in for instance TbMn_2O_5 the magneto-electric coupling is so strong that the electric polarization can be reversed by an external magnetic field [4]. This breakthrough can open new routes for the design of magneto-electric devices.

From a fundamental point of view, however, these multiferroic manganites contain a puzzle. In regular, nonmagnetic ferroelectrics the size of the macroscopic polarization P computed by modern *ab initio* band structure methods agrees exceptionally well with the ones observed experimentally [11]. In the multiferroic manganites, however, state of the art *ab initio* computations predict a P of around 1200 nC/cm^2 (Tb [12,13] and Ho), whereas the experimentally observed values are more than an order of magnitude smaller ($P = 45, 65, 100, \text{ and } 115 \text{ nC/cm}^2$ for Tb, Ho, Y, and Eu, respectively [4–10]). The question arises whether this large discrepancy is due to experimental artifacts, for instance the formation of ferroelectric domains, or due to an incompleteness in our understanding of the physical properties of these magnetic ferroelectric materials. The outcome of this puzzle is not only of fundamental interest, as large theoretical values of P promise experimentalists a boost of polarization upon enhanced material quality, increasing the multiferroics' application potential.

We will show in this Letter that the small polarization is intrinsic and caused by electronic correlations. It arises because the two contributions to P , the ionic part from the lattice displacements and the electronic part from the valence electrons are opposite and almost canceling each other. In this way, the electron-electron interactions drive a decimation of the resulting net polarization. We compute P to be in close agreement with the experimental value only

when the strong local Coulomb interactions between the manganese $3d$ electrons are accounted for.

Structure of RMn_2O_5 .—In the following, we will focus on the case $R = \text{Ho}$, but our conclusions are generic for this class of compounds. Neutron and x-ray diffraction studies show that these manganites have space group $Pb\bar{m}$, but it is expected that in their multiferroic state, the actual symmetry group is $Pb2_1m$, which allows for a macroscopic electric polarization along the b axis [5–7]. The orthorhombic $Pb\bar{m}$ crystal structure of HoMn_2O_5 consists of connected Mn^{4+}O_6 octahedra and Mn^{3+}O_5 pyramids (see Fig. 1). The octahedra share edges and form ribbons parallel to the c axis. Adjacent ribbons are linked by pairs of corner-sharing pyramids. Below 38 K HoMn_2O_5 , a commensurate magnetic structure develops with propagation vector $\mathbf{k} = (\frac{1}{2}, 0, \frac{1}{4})$, and simultaneously the system becomes ferroelectric [14].

We expand upon previous *ab initio* calculations by including the very strong local Coulomb interactions be-

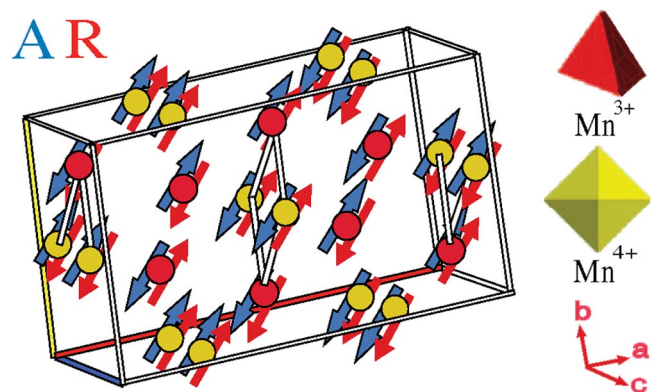


FIG. 1 (color online). Schematic view of the crystal structure of HoMn_2O_5 consisting of connected Mn^{4+}O_6 octahedra (right, middle) and Mn^{3+}O_5 pyramids (right, top). The magnetic structure of the ground state, labeled A, and its enantiomorphic counterpart, labeled R, are shown. The white bars connect Mn ions of the $\text{Mn}^{3+} - \text{Mn}^{4+} - \text{Mn}^{3+}$ structure along the b axis.

TABLE I. Computed structural parameters of HoMn_2O_5 in $Pb2_1m$ crystal structure using SGGA, SGGA + U . Distances are in Å; atoms occupying equivalent Wyckoff positions are shown only once.

| | $U = 0.0$ | | | $U = 8.0$ | | |
|------------------|-----------|--------|--------|-----------|--------|--------|
| | | | | | | |
| a, b, c | 14.5188 | 8.5271 | 5.6681 | 14.6847 | 8.5480 | 5.7858 |
| Ho^{3+} | 0.0693 | 0.1725 | 0 | 0.0690 | 0.1700 | 0 |
| | 0.3190 | 0.3278 | 0 | 0.3178 | 0.3300 | 0 |
| Mn^{4+} | 0 | 0.5003 | 0.2559 | 0.9996 | 0.4997 | 0.2536 |
| Mn^{3+} | 0.2032 | 0.3530 | 0.5 | 0.2063 | 0.3482 | 0.5 |
| | 0.4534 | 0.1485 | 0.5 | 0.4566 | 0.1533 | 0.5 |
| O_1 | 0.0004 | 0.0004 | 0.2702 | 0.0005 | 0.0004 | 0.2682 |
| O_2 | 0.0823 | 0.4447 | 0 | 0.0810 | 0.4415 | 0 |
| | 0.3324 | 0.0549 | 0 | 0.3317 | 0.0584 | 0 |
| O_3 | 0.0768 | 0.4305 | 0.5 | 0.0727 | 0.4242 | 0.5 |
| | 0.3275 | 0.0674 | 0.5 | 0.3238 | 0.0736 | 0.5 |
| O_4 | 0.1983 | 0.2075 | 0.2446 | 0.1955 | 0.2057 | 0.2382 |
| | 0.4471 | 0.2921 | 0.7571 | 0.4447 | 0.2942 | 0.7625 |

tween the manganese $3d$ electrons—the Hubbard U . We use the projector augmented-wave method (PAW) and plane wave basis sets as implemented in VASP [15]. Exchange and correlation are treated using the generalized gradient spin-density approximation [16] (SGGA) and the SGGA + U method [17,18]. We performed the SGGA + U calculations for $U = 4$ and 8 eV and a Hund’s rule exchange of $J_H = 0.88$ eV for the Mn d -electrons, in the range of values that were obtained from constrained density functional calculations on perovskite manganites (~ 10 eV) in Ref. [19] and from the analysis of photoemission spectroscopy (4–5 eV) [20,21]. Using two different values of U allows us to investigate the trend of the polarization when the strength of electronic correlations is increased.

Starting from the experimental centrosymmetric $Pbam$ crystal structure, we relax unit cell parameters and ionic positions both in the SGGA and SGGA + U schemes, allowing for the lower symmetry $Pb2_1m$ structure to develop. The atomic positions are relaxed in a $2 \times 1 \times 1$ magnetic super cell (containing 64 ions) along the magnetic k_x direction [22]. We find that the experimental magnetic structure of HoMn_2O_5 (labeled by A in Fig. 1) with $Pb2_1m$ symmetry is indeed the magnetic ground state. The calculated structural parameters for $U = 0$ and $U = 8$ are shown in Table I. They are in good agreement with both the experimental data and first principles electronic structure computations on TbMn_2O_5 without correlations [7,12,13]. The ionic displacements are small but significant, in agreement with the fact that experimentally the low symmetry structure cannot directly be determined [14]. In Table II, we report the computed band gap Δ and energy gain due to the ferroelectric distortion δE_{FE} (see Fig. 3).

Ferroelectric atomic displacements.—The relaxation results in Mn^{3+} and O_3 have significant atomic displacements

TABLE II. Gap Δ , energy gain of the ferroelectric state δE_{FE} and Born effective charges of different manganese ions in multi-ferroic HoMn_2O_5 with $Pb2_1m$ symmetry within SGGA and SGGA + U .

| U (eV) | Δ (eV) | δE_{FE} (meV) | $\text{Mn}_{\uparrow}^{3+}$ | $\text{Mn}_{\uparrow}^{4+}$ | $\text{Mn}_{\downarrow}^{3+}$ |
|----------|---------------|------------------------------|-----------------------------|-----------------------------|-------------------------------|
| 0.0 | 0.5 | 26.4 | 3.85 | 4.74 | 4.17 |
| 4.0 | 1.6 | 12.1 | 3.94 | 4.03 | 4.08 |
| 8.0 | 1.6 | 18.6 | 3.69 | 3.65 | 3.87 |

along the b direction, compared to which the displacements for other ions and in other directions are small. In Fig. 2, the displacements of these two types of atoms are indicated. In the a and c direction, the ionic displacements are mirror symmetric so that they will not contribute to developing a ferroelectric polarization.

One qualitative difference between the relaxed unit cells obtained in SGGA and SGGA + U appears in the oxygen octahedra surrounding the Mn^{4+} ions: SGGA calculations show that the Mn^{4+} move along the b direction and become off-centered (the bonds along the longest axis of the octahedron become 1.921 and 1.935 Å, respectively) while switching on the Coulomb interaction U results in a suppression of this off-centering. The effect is not unexpected as the inclusion of the electronic correlations increases the band gap significantly, rendering the electronic system more rigid and less susceptible to perturbations. The instability to off-centering is well known to be related to the hybridization of the transition metal $3d$ states with the oxygen $2p$ states [1,23]. Increasing U leads to a larger gap, a larger splitting between occupied oxygen p , and empty Mn d states and therefore a smaller effective hybridization between the two.

Along the b -direction, HoMn_2O_5 exhibits a charge and spin ordering that can schematically be denoted as a chain of $\text{Mn}_{\uparrow}^{3+} - \text{Mn}_{\uparrow}^{4+} - \text{Mn}_{\downarrow}^{3+}$, see Fig. 2. In the undistorted $Pbam$ structure, the distances $d_{\uparrow\uparrow}$ (between $\text{Mn}_{\uparrow}^{3+}$ and $\text{Mn}_{\uparrow}^{4+}$) and $d_{\downarrow\uparrow}$ (between $\text{Mn}_{\downarrow}^{3+}$ and $\text{Mn}_{\uparrow}^{4+}$) are the same. Relaxation reveals a shortening of distances between parallel spins $\text{Mn}_{\uparrow}^{3+}$ and $\text{Mn}_{\uparrow}^{4+}$ ions: in the ferroelectric

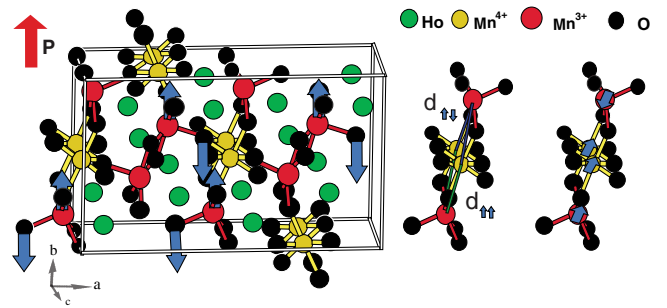


FIG. 2 (color online). Left: arrangement of the ions in the unit cell with arrows indicating the ionic displacements of Mn^{3+} and O_3 . Right: schematic view of the magnetic and charge ordered $\text{Mn}_{\uparrow}^{3+} - \text{Mn}_{\uparrow}^{4+} - \text{Mn}_{\downarrow}^{3+}$ arrangement along the b direction.

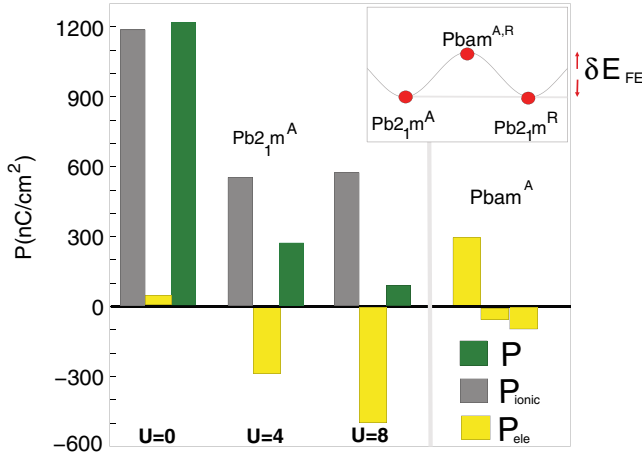


FIG. 3 (color online). Ionic, electronic, and total polarization for different values of U in the relaxed $Pb_{21}m$ structure (left) and P_{ele} in the $Pbam$ structure (right). Inset: ferroelectric energy gain, δE_{FE} .

$Pb_{21}m$ structure $d_{\uparrow\uparrow} < d_{\downarrow\uparrow}$, which optimizes the double exchange energy [3,24].

Ionic and electronic polarization.—The total polarization P for a given material is the sum of the ionic polarization P_{ion} and electronic one P_{ele} [11,25]. In our *ab initio* calculations, the ionic contribution P_{ion} is easily obtained by summing the product of the ionic displacements from the centrosymmetric to the ferroelectric structure with the nominal charge of the ions' rigid core. To calculate the electronic contribution P_{ele} , we use the Berry phase method developed by King-Smith and Vanderbilt within the PAW formalism [26].

First, we consider the magnetically ordered *high symmetry* $Pbam$ phase of HoMn_2O_5 , in which by definition $P_{\text{ion}} = 0$. The electronic part to the polarization, however, is not required to vanish. In fact, the material is bound to have a magnetically induced ferroelectric polarization as it is a dislocated spin-density wave system in which the center of symmetry of the magnetic and lattice structure do not coincide, providing a basic mechanism for multiferroicity [10,27]. An equivalent point of view is that symmetry allows for a purely electronic part to the magnetostriction [3,28]. As a consequence, the spin ordering induces a redistribution of charge on crystallographically inequivalent manganese sites.

We find in the centrosymmetric A structure a resulting polarization of $P_{\text{ele}} = 284 \text{ nC/cm}^2$ along the b axis for $U = 0$. We checked that inverting all the spins, producing the reversed (R) $Pbam$ structure, leads to the same polarization in opposite direction. A finite U alters the ferroelectric charge redistribution and gives rise to a polarization $P_{\text{ele}} = -14 / -81 \text{ nC/cm}^2$ for $U = 4/8 \text{ eV}$ in the A spin structure [29]. The fact that P_{ele} is induced by the magnetic superstructure is immediately clear from a computation on this system in the ferromagnetic state, in which we find all polarization to vanish.

In the results above, it is remarkable that the electronic correlation effects induce a sign change of P_{ele} . This is a real effect caused by changes in electronic structure and is not related to geometric constraints in our calculations. A polarization flip is possible because symmetry considerations alone do not fix the sign of the magnetically induced polarization—the sign of the magneto-electric coupling. Thus, an inversion of the polarization as a function of U is symmetry allowed, just as a temperature induced sign change of the coupling is possible and indeed observed in some materials [30]. At the end of this Letter, we present the microscopic mechanism behind this correlation induced polarization flip.

In the relaxed $Pb_{21}m$ structure, the ionic contribution to the polarization comes into play. We find $P_{\text{ion}} = 1193/546/576 \text{ nC/cm}^2$ for $U = 0/4/8$, concomitant with an electronic polarization $P_{\text{ele}} = 12 / -287 / -493 \text{ nC/cm}^2$, resulting in a total polarization $P = 1205/259/82 \text{ nC/cm}^2$ in the magnetic A structure [29]. These values are shown in Fig. 3. The value of the polarization for $U = 8$ is in very good agreement with experiment. From the computed values of P_{ion} and P_{ele} , we conclude that the Hubbard U causes a near cancellation of the electronic and ionic contributions to the polarization and effectively reduces the polarization in the multiferroic manganites by over an order of magnitude.

Origin of the near cancellation.—The ionic contribution to the polarization is driven by the fact that (i) the interatomic Mn distances depend on spin direction ($d_{\uparrow\uparrow} < d_{\downarrow\uparrow}$), and (ii) the valence of the two Mn ions approaching each other is different, see left panel of Fig. 4. Electronic correlations reduce P_{ion} by a factor of 2, due to the increased electronic rigidity which reduces atomic displacements, see Fig. 3. In spite of this correlation induced reduction, the computed P_{ion} is still about 6 times larger than the experimental polarization P .

The electronic polarization P_{ele} arises from a reorganization of valence charges caused by both ferroelectric lattice distortions and magnetic ordering. Both these cause changes in covalency, which in turn cause a flow of valence electron charge across the material. Therefore, the effec-

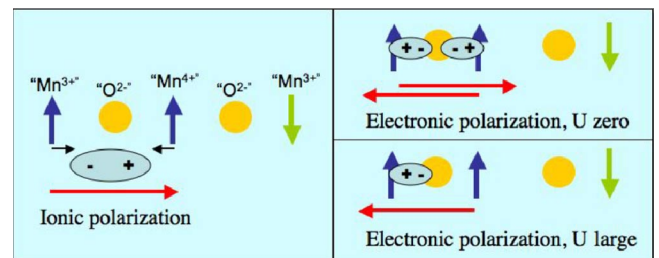


FIG. 4 (color online). Schematic view of the two contributions to the ferroelectric polarization in HoMn_2O_5 in the uncorrelated ($U = 0$) and strongly correlated limit (large U). In the latter, the electronic polarization nearly cancels the ionic polarization. The labels “ $\text{Mn}^{4+/3+}$ ” indicate Mn ions that have a valence of more/less than $3.5+$, respectively.

tive charge that is displaced by a distortion can be much larger than just the bare ionic value. We computed this Born effective charges of the Mn ions along the $\text{Mn}_{\uparrow}^{3+} - \text{Mn}_{\downarrow}^{4+} - \text{Mn}_{\uparrow}^{3+}$ direction in the ferroelectric $Pb2_1m$ structure, see Table II.

When $U = 0$, all Born charges are larger than the nominal ones, indicative of the distortions inducing appreciable changes in covalency. The microscopic mechanism is that both the $\text{Mn}_{\uparrow}^{4+}$ and $\text{Mn}_{\uparrow}^{3+}$ ions transfer charge to the oxygen atoms connecting them when they move closer together, see Fig. 4. In this situation, the electrons gain kinetic energy because they can hop between $\text{Mn}_{\uparrow}^{4+}$ and $\text{Mn}_{\uparrow}^{3+}$ without violating the on-site Hund's rule [24]. The induced electronic polarizations (Fig. 4) are opposite and cancel each other, in agreement with the very small $P_{\text{ele}} = 12 \text{ nC/cm}^2$ that we find in $Pb2_1m$ when $U = 0$.

When U is large, the situation changes drastically. The system becomes more ionic, depleting valence charge from the Mn^{4+} sites, which approaches a closed shell t_{2g}^3 configuration, and increasing it at the Mn^{3+} sites. Covalency of the Mn-O bonds of the former will therefore be strongly reduced at the expense of the latter, see Fig. 4. Indeed, we see in Table I that the electronic correlations push the Born effective charge of Mn^{4+} below even its nominal value of $4+$.

Conclusions.—The overall result is that in these strongly correlated multiferroic manganites, a large electronic polarization develops, which is almost as large as the ionic polarization, but opposite in direction, see Fig. 4. An intrinsically small net polarization of $P = 82 \text{ nC/cm}^2$ results, in very good agreement with the experimental value. We therefore conclude that electron-electron interactions decimate the polarization in the multiferroic RMn_2O_5 manganites. Electronic correlation effects are thus of prime importance and quantitatively dominate the physical properties of these multiferroic transition metal compounds.

We thank Claude Ederer, Nicola Spaldin, Maxim Mostovoy, and Silvia Picozzi for fruitful discussions. We thank Lixin He for detailed discussions on TbMn_2O_5 . This work was financially supported by *NanoNed*, a nanotechnology programme of the Dutch Ministry of Economic Affairs and by the Nederlandse Organisatie voor Wetenschappelijk Onderzoek (NWO) and the Stichting voor Fundamenteel Onderzoek der Materie (FOM). Part of the calculations were performed with a grant of computer time from the Stichting Nationale Computerfaciliteiten (NCF).

[1] N. A. Hill, *J. Phys. Chem. B* **104**, 6694 (2000).

[2] D. I. Khomskii, *J. Magn. Magn. Mater.* **306**, 1 (2006).

- [3] S. W. Cheong and M. Mostovoy, *Nat. Mater.* **6**, 13 (2007).
- [4] N. Hur, S. Park, P. A. Sharma, J. S. Ahn, S. Guba, and S. W. Cheong, *Nature (London)* **429**, 392 (2004).
- [5] I. Kagomiya *et al.*, *Ferroelectrics* **286**, 167 (2003).
- [6] L. C. Chapon *et al.*, *Phys. Rev. Lett.* **93**, 177402 (2004).
- [7] J. Alfonso *et al.*, *J. Phys. Condens. Matter* **9**, 8515 (1997).
- [8] N. Hur *et al.*, *Phys. Rev. Lett.* **93**, 107207 (2004).
- [9] D. Higashiyama, S. Miyasaka, and Y. Tokura, *Phys. Rev. B* **72**, 064421 (2005).
- [10] L. C. Chapon *et al.*, *Phys. Rev. Lett.* **96**, 097601 (2006).
- [11] *Physics of Ferroelectrics: A Modern Perspective*, edited by K. M. Rabe, C. H. Ahn, and J.-M. Triscone (Springer, Berlin, 2007).
- [12] C. Wang, G.-C. Guo, and L. He, *Phys. Rev. Lett.* **99**, 177202 (2007).
- [13] C. Wang, G.-C. Guo, and L. He, *Phys. Rev. B* **77**, 134113 (2008).
- [14] G. R. Blake *et al.*, *Phys. Rev. B* **71**, 214402 (2005).
- [15] G. Kresse and J. Furthmüller, *Phys. Rev. B* **54**, 11169 (1996); *Comput. Mater. Sci.* **6**, 15 (1996).
- [16] J. P. Perdew *et al.*, *Phys. Rev. B* **46**, 6671 (1992); **48**, 4978 (1993).
- [17] A. Rohrbach, J. Hafner, and G. Kresse, *Phys. Rev. B* **69**, 075413 (2004).
- [18] A. I. Liechtenstein, V. I. Anisimov, and J. Zaanen, *Phys. Rev. B* **52**, R5467 (1995).
- [19] S. Satpathy, Z. S. Popovic, and F. R. Vukajlovic, *Phys. Rev. Lett.* **76**, 960 (1996).
- [20] J.-H. Park *et al.*, *Phys. Rev. Lett.* **76**, 4215 (1996).
- [21] T. Geng and S. Zhuang, *Phys. Lett. A* **372**, 533 (2008).
- [22] We use a cutoff energy of 500 eV to expand the pseudo wave functions and a $2 \times 6 \times 8$ k -point mesh combined with the use of tetrahedron method to integrate the Brillouin zone. The relaxation is continued until the changes of total energy were less than 10^{-7} eV, resulting in Hellmann-Feynman forces smaller than 1 meV/\AA . To calculate the electronic contribution to the polarization, we used 14 k -points for each “string” along the b direction.
- [23] A. Filippetti and N. A. Spaldin, *Phys. Rev. B* **68**, 045111 (2003).
- [24] D. V. Efremov, J. van den Brink, and D. I. Khomskii, *Nat. Mater.* **3**, 853 (2004).
- [25] R. Resta, *Rev. Mod. Phys.* **66**, 899 (1994).
- [26] R. D. King-Smith and D. Vanderbilt, *Phys. Rev. B* **47**, 1651 (1993); D. Vanderbilt and R. D. King-Smith, *Phys. Rev. B* **48**, 4442 (1993).
- [27] J. J. Betouras, G. Giovannetti, and J. van den Brink, *Phys. Rev. Lett.* **98**, 257602 (2007).
- [28] A. B. Harris, *Phys. Rev. B* **76**, 054447 (2007).
- [29] We checked that the inverted R magnetic structure leads to a polarization in the opposite direction with the same amplitude and have the same ground-state energy.
- [30] S. W. Cheong (private communication).